Eur. Phys. J. D (2013)
DOI: 10.1140/epjd/e2013-30714-5

THE EUROPEAN PHYSICAL JOURNAL D

Regular Article

The study of the 4s4p configuration of the Zn isoelectronic sequence using the relativistic jj-coupling approach

J.C. Aguiar[1], M. Raineri[2], and H.O. Di Rocco[3,4,a]

[1] Autoridad Regulatoria Nuclear, Av. del Libertador 8250, C1429BNP Buenos Aires, Argentina
[2] Centro de Investigaciones Ópticas, CC 3, 1897 Gonnet, La Plata, Argentina and Comisión de Investigaciones Científicas, La Plata, Argentina
[3] Instituto de Física Arroyo Seco, Facultad de Ciencias Exactas, Universidad Nacional del Centro, Pinto 399, 7000 Tandil, Argentina
[4] Consejo Nacional de Investigaciones Científicas y Técnicas (CONICET), Argentina

Received 28 November 2012 / Received in final form 26 February 2013
Published online (Inserted Later) – © EDP Sciences, Società Italiana di Fisica, Springer-Verlag 2013

Abstract. The $4s4p$ configuration of Zn is analyzed using the *Relativistic jj-coupling approach*. The experimentally determined relativistic Slater integrals are compared with the results of numerical codes, both quasi- and fully-relativistic ones. In this work, they are estimated, semi-empirically, the two $J = 1$ levels up $Z = 70$ and the $^1P_1$ level up $Z = 92$ by judicious interpolation and extrapolation of energies. The comparison with extensive relativistic configuration-interaction calculations indicates that differences between both approaches are of the order of measurement accuracies.

1 Introduction

The $4s4p$ configuration of the Zn isoelectronic sequence is one of the most profusely studied atomic systems; in fact, it was analyzed from the experimental, as well as the theoretical and semi-empirical approaches. A complete bibliography can be found at the web site of the NIST [1].

From the experimental point of view diverse spectroscopic sources were used. Leaving aside the old works, referenced in the NIST web page, from 1980 to date, the most extensive ones are: Reader and Luther [2], using laser produced plasmas (LPP), Acquista and Reader (LPP) [3], Isberg and Litzén [4] (hollow-cathode), Joshi and van Kleef [5] (triggered spark), Trigueiros et al. [6] (theta-pinch), Hinnov et al. [7] (tokamak), Litzén and Reader [8] (low-inductance vacuum spark), Churilov and Ryabtsev [9] (LPP), Sugar et al. [10] (tokamak), Ryabtsev et al. [11] (triggered three-electrode vacuum spark), Brown et al. [12] (LPP), Churilov and Joshi [13] (triggered spark and a sliding spark source), Träbert et al. [14,15] (EBIT). The general panorama is that the four levels of the $nsnp$ configuration are known up to $Z = 50\,(Z_c = 21)$; the two $J = 1$ levels are known (with holes) up to $Z = 70$ $(Z_c = 41)$, whereas the $^1P_1$ level is measured (with holes) up to $Z = 92\,(Z_c = 63)$.

From the theoretical point of view, this sequence was analyzed with the quasi-relativistic approach using the codes of Cowan [16] and Froese Fischer [17], as well as fully-relativistic approaches using the HULLAC [12] and the GRASP [18] codes. Several extensive calculations appeared in diverse Journals and the complete list can be found in reference [1].

The semi-empirical method, widely developed and used by Edlén, and presented in their famous article [19] was continued with success by Curtis and condensed in their book [20]. In particular, a study of the Zn sequence was published by Curtis in 1985 (Ref. [21]). The experimental material was limited to $Z = 42\,(Zc = 13)$ for the four levels, and up to $Z = 56$ for the $^1P_1$ level. In a number of cases, some of the levels used by Curtis were corrected in new analysis made after that year.

The general purpose of this work is to do a similar study as the one made by Curtis but using the new experimental material collected up to the present and using the *jj-coupling Relativistic Theory*. The authors working with the non-relativistic codes [16,17] present the comparison between theoretical Slater and spin-orbit integrals with the values deduced from the experiments. But this is not so when using fully-relativistic codes [12,29,30]. Therefore, one of our specific purposes is to make the comparison between the experimentally deduced Slater parameters and those provided by the GRASP code generated by ourselves. The second specific purpose is to use the capability of the semi-empirical method for interpolation, extrapolation and consistency checking. So, the establishment of missing $^1P_1$ and $^3P_1$ levels (eleven in the range $Z = 51$–69) will be presented. Also, from the new measurements of

[a] e-mail: hdirocco@exa.unicen.edu.ar

Träbert et al. [14,15] for $Z = 70, 74, 76, 78, 79, 82, 83, 90$ and 92, the level $^1\mathrm{P}_1$ is predicted, ultimately, for the entire isoelectronic sequence.

2 Theory

In the non-relativistic approach, the average energy of the $nsnp$ configuration can be written in the form [22]:

$$E_{AV} = E(cs) + E(cs, ns) + E(cs, np) + F^0(ns, np) - \frac{G^1(ns, np)}{2(2l+1)}, \quad (1)$$

where $E(cs)$ is written for interactions of the pairs of electrons in closed shells, plus their $I(nl)$ one-electron integrals, $E(cs, nl)$ is the interaction of the nl electron with those in closed shells, $F^0(ns, np)$ and $G^1(ns, np)$ are the Slater integrals. Furthermore, the singlet and triplet energies are referred to E_{AV} as $^1\mathrm{P} = G^1(ns, np)/2$ and $^3\mathrm{P} = -G^1(ns, np)/6$. Similar expressions can be written for the relativistic case.

The $4s4p$ configuration gives four levels that are designed, in the LS and jj schemes as:

$$\begin{array}{lcl} \textit{LS-coupled states} & & \textit{jj-coupled states} \\ nsnp\,^1\mathrm{P}_1 & \longleftrightarrow & \left(ns_{1/2}np_{3/2}\right)1 \\ nsnp\,^3\mathrm{P}_2 & \longleftrightarrow & \left(ns_{1/2}np_{3/2}\right)2 \\ nsnp\,^3\mathrm{P}_1 & \longleftrightarrow & \left(ns_{1/2}np_{1/2}\right)1 \\ nsnp\,^3\mathrm{P}_0 & \longleftrightarrow & \left(ns_{1/2}np_{1/2}\right)0 \end{array} \quad (2)$$

resulting that, for low Z values, the levels are grouped in a singlet and a triplet, whereas for high Z they are grouped in two pairs: $(ns_{1/2}np_{3/2})$ and $(ns_{1/2}np_{1/2})$.

Briefly, the *Non-relativistic coupling schema* in general, and their LS and jj approximations can be found in references [19,20]. In the case of our present interest, the four energy levels can be characterized by three parameters: E_0 (that contains F^0), $G^1(sp)$ and the *spin-orbit* integral ζ_p. Important consequences of the non-relativistic treatment are exactly

$$E\left(^3\mathrm{P}_2\right) - E\left(^3\mathrm{P}_0\right) = 3\zeta_p/2 \quad (3)$$

and

$$1.5\left[\left(E\left(^1\mathrm{P}_1\right) + E\left(^3\mathrm{P}_1\right)\right) - \left(E\left(^3\mathrm{P}_2\right) + E\left(^3\mathrm{P}_0\right)\right)\right] = G^1(sp); \quad (4)$$

departing from the election made by Curtis (see Ref. [21]). It is important to remark that, as there are two energy parameters ($G^1(sp)$ and ζ_p) in the non-relativistic treatment, the system is overdeterminated, and Dr. Curtis removed such overdeterminacy by using, only for parametrization purposes, two values for $G^1(sp) : G^1_A(sp)$ and $G^1_B(sp)$ arising from different level intervals. A similar analysis was applied to the *Sm* isoelectronic sequence [23].

2.1 Relativistic jj coupling

The theory for the Relativistic jj coupling can be viewed in detail in a previous paper written by one of us [24], based in the book by Shore and Menzel [25], conveniently modified to introduce the relativistic Slater integrals $G^1\left(ns_{1/2}, np_{1/2}\right)$ and $G^1\left(ns_{1/2}, np_{3/2}\right)$ in the place of $G^1(ns, np)$. Other presentations can be found in the book by de-Shalit and Talmi about the nuclear shell model [26] or in an article by Larkins [27]. Lamentably, in these last two cases, it is not taken into account the interaction between the two $J = 1$ levels (called *the breaking of the jj coupling* by Shore and Menzel). A modern presentation can be found in the books by Grant [18] and Johnson [28]. The direct elements are

$$\begin{aligned} \left\langle abJM \left| r_{12}^{-1} \right| a'b'JM \right\rangle = \sum_k (-1)^{J+j_b-j'_b+1+l_a+l_b} \\ \times \left\{[j_a]\,[j'_a]\,[j_b]\,[j'_b]\right\}^{1/2} \\ \times S_{6j}\left(J, j_b, j_a; k, j'_a, j'_b\right) \\ \times S_{6j}\left(1/2, j_a, l_a; k, l'_a, j'_a\right) \\ \times S_{6j}\left(1/2, j_b, l_b; k, l'_b, j'_b\right) \\ \times \left\langle l_a \left\| \mathbf{C}^{(k)} \right\| l'_a \right\rangle \\ \times \left\langle l_b \left\| \mathbf{C}^{(k)} \right\| l'_b \right\rangle R^k(ab, a'b') \end{aligned} \quad (5)$$

with the abbreviated notation

$$[j_1, j_2, \ldots] \equiv (2j_1+1)(2j_2+1)\ldots$$

and with S_{6j} we indicate the $6j$ symbol; $\mathbf{C}^{(k)}$ indicates the Racah spherical tensor. The exchange contribution leads to the elements

$$\begin{aligned} \left\langle abJM \left| r_{12}^{-1} \right| b'a'JM \right\rangle = \sum_k (-1)^{2J+2j_b+j_a-j'_a+2} \\ \times \left\{[j_a]\,[j'_a]\,[j_b]\,[j'_b]\right\}^{1/2} \\ \times S_{6j}\left(J, j_b, j_a; k, j'_b, j'_a\right) \\ \times S_{6j}\left(1/2, j_a, l_a; k, l'_b, j'_b\right) \\ \times S_{6j}\left(1/2, j_b, l_b; k, l'_a, j'_a\right) \\ \times \left\langle l_a \left\| \mathbf{C}^{(k)} \right\| l'_b \right\rangle \\ \times \left\langle l_b \left\| \mathbf{C}^{(k)} \right\| l'_a \right\rangle R^k(ab, b'a'). \end{aligned} \quad (6)$$

The energy levels can be written, using both the jj notation and LS (for usefulness), as:

$$^3\mathrm{P}_0 \equiv (1/2, 1/2)_0 \quad = E_0(sp_-) - G^1(sp_-)/3 \quad (7)$$

$$^3\mathrm{P}_2 \equiv (1/2, 3/2)_2 \quad = E_0(sp_+) - G^1(sp_+)/3 \quad (8)$$

whereas $^3\mathrm{P}_1$ and $^1\mathrm{P}_1$ levels arise from the diagonalization of the matrix

$$\left\| \begin{array}{cc} A & C \\ C & B \end{array} \right\| \equiv \left\| \begin{array}{cc} E_0(sp_+) + G^1(sp_+)/9 & \sqrt{8}R^1(sp_-, sp_+)/9 \\ \sqrt{8}R^1(sp_-, sp_+)/9 & E_0(sp_-) - G^1(sp_-)/9 \end{array} \right\|. \quad (9)$$

From equation (9), the expressions for the eigenvalues are given by:

$$
\begin{aligned}
{}^3\mathrm{P}_1 = &\left\{ \frac{1}{2}\left[E_0\left(sp_-\right) + E_0\left(sp_+\right)\right] \right. \\
&\left. + \frac{1}{18}\left[-G^1\left(sp_-\right) + G^1\left(sp_+\right)\right] \right\} \\
&- \frac{1}{18}\Big\{ \left[G^1\left(sp_-\right) + G^1\left(sp_+\right) + 9E_0\left(sp_+\right)\right. \\
&\left. - 9E_0\left(sp_-\right)\right] \hat{}\, 2 + 32\left(R^1\left(sp_-, sp_+\right)\right)^2 \Big\}^{1/2} \qquad (10)
\end{aligned}
$$

and

$$
\begin{aligned}
{}^1\mathrm{P}_1 = &\left\{ \frac{1}{2}\left[E_0\left(sp_-\right) + E_0\left(sp_+\right)\right] \right. \\
&\left. + \frac{1}{18}\left[-G^1\left(sp_-\right) + G^1\left(sp_+\right)\right] \right\} \\
&+ \frac{1}{18}\Big\{ \left[G^1\left(sp_-\right) + G^1\left(sp_+\right) + 9E_0\left(sp_+\right)\right. \\
&\left. - 9E_0\left(sp_-\right)\right] \hat{}\, 2 + 32\left(R^1\left(sp_-, sp_+\right)\right)^2 \Big\}^{1/2}. \qquad (11)
\end{aligned}
$$

Note that for prediction purposes valid for high Z values, the eigenvalues of equation (9) when $C/\left(A-B\right) \ll 1$, simplify very approximately to (see Ref. [16], p. 290)

$$
{}^1\mathrm{P}_1 \approx A + \frac{C^2}{A-B} - \frac{C^4}{\left(A-B\right)^3}
$$

and

$$
{}^3\mathrm{P}_1 \approx B - \frac{C^2}{A-B} + \frac{C^4}{\left(A-B\right)^3}.
$$

Explicitly

$$
\begin{aligned}
{}^1\mathrm{P}_1 \approx &\left[E_0\left(sp_+\right) + \frac{G^1\left(sp_+\right)}{9}\right] \\
&+ \frac{8\left(R^1\right)^2/81}{\left[E_0\left(sp_+\right) - E_0\left(sp_-\right)\right] + \left[G^1\left(sp_+\right) + G^1\left(sp_-\right)\right]/9}. \qquad (12)
\end{aligned}
$$

The expresion (12) will be used below to find the ${}^1\mathrm{P}_1$ values for $Z > 72$ (up to $Z = 92$).

In this work we adopted $E_0\left(sp_-\right)$ and $E_0\left(sp_+\right)$ so that the level energies are measured with respect to the ground level $4s^2\ {}^1\mathrm{S}_0 = 0$, and not with respect to average energies. We chose this convention, as opposed to measure with respect to $E_{AV}(sp_-)$ and $E_{AV}(sp_+)$ because we know the four levels only up to $Z = 50$; therefore, it is not possible to use the E_{AV}'s for higher Z, but it is possible to use the E_0's. The property mentioned in equation (4) for the non-relativistic case is now

$$
\begin{aligned}
1.5\left[\left(E\left({}^1\mathrm{P}_1\right) + E\left({}^3\mathrm{P}_1\right)\right) - \left(E\left({}^3\mathrm{P}_2\right) + E\left({}^3\mathrm{P}_0\right)\right)\right] \\
= \frac{G^1\left(sp_-\right)}{3} + \frac{2G^1\left(sp_+\right)}{3},
\end{aligned}
$$

such that

$$
3G^1\left(sp\right) = G^1\left(sp_-\right) + 2G^1\left(sp_+\right). \qquad (13)
$$

Because the Slater integrals $G^1(sp)$ and $R^1(sp_-, sp_+)$, multiplied by their respective factors, are much lower that $E_0(sp_-)$ and $E_0(sp_+)$, it is confirmed that for high Z values the energy levels tend to appear in pairs: $(1/2, 1/2)_{0,1}$ and $(1/2, 3/2)_{1,2}$, as it is in the jj non-relativistic case [19,20].

It must be taken into account that we obtain effective relativistic Slater parameters in practice, because we are not introducing neither Breit nor QED contributions in our model. Such contributions to the excitation energies were calculated theoretically in references [29,30]. In the work of Chen and Cheng [29], it is shown that self-energy (SE) corrections are the most important contributions to QED effects. It is interesting to note that, concerning to these QED corrections, we verified that the explicit functional approximations developed by Curtis for self-energy [31] produce good qualitative results (within 18% for high Z) for $E(4p_{1/2}) - E(4p_{3/2})$ differences. Curtis presented their SE parametrization written as:

$$
E_{nlj}\left(Z\right) = \frac{2R\alpha^3 Z^4}{\pi n^3} F_{nlj}\left(Z\right) \qquad (14)
$$

in order to see the dominant Z and n dependences. $F_{nlj}(Z)$ is the reduced splitting factor and Curtis used exact calculations and developed explicit formulae useful in the semi-empirical study of isoelectronic sequences (see Eq. (17) below).

Comparing with the Chen and Cheng QED corrections for the Zn sequence, it is interesting to see that the simple screened-hydrogen model of Curtis is accurate enough, even when devised primarily for alkali-like one-electron spectra. For our estimations, we used effective charges Z_{eff} for the $4s$, $4p_{1/2}$ and $4p_{3/2}$ orbitals. From the expectation values $\langle r\rangle$, $\langle r^2\rangle$ and $\langle 1/r\rangle$ provided by the GRASP code we inferred Z_{eff} values supposing screened hydrogenic orbitals. Despite the roughness of the method, we present our estimations, as well as the Chen and Cheng values [29] at the end of Section 5, in order to show such good agreement.

3 The correlation between the experimental data and the theoretical parameters

As it was said above, the four levels of the $4s4p$ configuration are known up to $Z = 50\,(Z_c = 21)$; the two $J = 1$ levels are known (with some holes) up to $Z = 70\,(Z_c = 41)$, whereas the ${}^1\mathrm{P}_1$ level was measured (with many holes) up to $Z = 92\,(Z_c = 63)$. Levels ${}^3\mathrm{P}_{0,2}$ do not decay to the fundamental $4s^2\ {}^1\mathrm{S}_0$, and there are unknown combinations with upper configurations (e.g. $4s4d$ or $4p^2$) for $Z > 50$; therefore, there are not experimental ${}^3\mathrm{P}_{0,2}$ values for $Z > 50$.

In general, the measurements for high Z values, provided by the different authors and different spectroscopic

sources, are discordant. Assuming, as an average, uncertainties in the wavelength measurements of the order of $\Delta\lambda \sim 0.01$ Å, it signifies that for $Z \sim 50$, where $\lambda \sim 200$ Å, we will have $\Delta\sigma \sim 25$ cm^{-1}, whereas that, for $Z = 92$, where $\lambda \sim 26$ Å, it implies $\Delta\sigma \sim 1500$ cm^{-1}. However, for $Z = 92$, the discrepance between the measurements given by different authors is about 5000 cm^{-1} (compare Refs. [12,14]).

It is very important to remark, for comparison purposes, that the laser-plasma results appear to drift to higher and higher energies as Z increases. The same trend is found in the $4s$–$4p$ transition energies in Cu-like ions where laser-plasma results are systematically higher than high-precision EBIT measurements and RCI calculations [29]. Therefore, we do not use the results from Brown et al. [12] for $Z \geq 70$ but the measurements from Träbert et al. [14,15].

3.1 Range Z = 30–50

When all levels of the configuration $nsnp$ are known, the theoretical parameters can be obtained without the use of numerical codes, if we take into account several properties of the relativistic treatment, because there are more parameters than in the non-relativistic case (see Ref. [20]). Indeed, in the place of E_0, we have now $E_0(sp_-)$ and $E_0(sp_+)$ and in the place of $G^1(sp)$ we have $G^1(sp_-)$ and $G^1(sp_+)$; furthermore, the interaction parameter $R^1(sp_-, sp_+)$ appears, but ξ_p does not appear. Because there are four levels and five parameters, we need one link equation. To this purpose, we use the relation (not the absolute numbers!) $G^1(sp_-)/G^1(sp_+) = 1.012$ provided by the GRASP code, a practically constant value in the complete sequence, from Zn^{0+} up to U^{62+}.

Therefore, in the range $Z = 30$–50, the values of $E_0(sp_-)$, $E_0(sp_+)$, $G^1(sp_-)$, $G^1(sp_+)$ and $R^1(sp_-, sp_+)$ are deduced from the experimental level values following these steps:

1) we calculate the non-relativistic value $G^1(sp)$ from equation (4),
2) using equation (13) and $G^1(sp_-) = 1.012\ G^1(sp_+)$ from the GRASP code, we calculate $G^1(sp_-)$ and $G^1(sp_+)$ as $G^1(sp_-) = 1.008\ G^1(sp)$ and $G^1(sp_+) = 0.996\ G^1(sp)$,
3) $E_0(sp_-)$ and $E_0(sp_+)$ are calculated from equations (7) and (8), respectively,
4) finally, $R^1(sp_-, sp_+)$ is calculated by diagonalizing equation (9) or by using any of the equations (10) or (11). In practice, $R^1(sp_-, sp_+) \cong G^1(sp)$ within 0.5%, as it must be expected from the relativistic ($Z = 1$) values, calculated as in reference [22].

After the calculations for $Z = 30$–50, we can fit the behavior of the relativistic Slater integrals $G^1(sp_-)$, $G^1(sp_+)$ and $R^1(sp_-, sp_+)$ with Z_c through the functional relations as follows:

$$\begin{aligned} G^1(sp_-)\big|_{EXPE} &= 5641.77Z_c + 33131.00 \\ &\quad - 21929.65\exp(-Z_c/2.62288) \\ &\quad - 20891.54\exp(-Z_c/0.47458) \\ G^1(sp_+)\big|_{EXPE} &= 5574.60Z_c + 33736.53 \\ &\quad - 21668.60\exp(-Z_c/2.62288) \\ &\quad - 20642.83\exp(-Z_c/0.47458) \\ R^1(sp_-, sp_+)\big|_{EXPE} &= 5526.30Z_c + 34573.90 \\ &\quad - 16485.56\exp -Z_c/3.839 \\ &\quad - 16589\exp(-Z_c/1.02574) \end{aligned} \quad (15)$$

essential for extrapolations for $Z \geq 51$; the goodness of these fits is shown in Table 1. On the other hand, the behavior of $E_0(sp_-)$ and $E_0(sp_+)$ has more complicated patterns. However, the difference $E_0sp_+) - E_0(sp_-)$ can be very well fitted and permits a judicious extrapolation for $Z \geq 51$.

All the adjustments given by equation (15) have the following remarkable property: the $A's$ coefficients are all very similar between them and similar to the hydrogenic values $G^1_H(sp_-)$, $G^1_H(sp_+)$ and $R^1_H(sp_-, sp_+)$, all of them of the order of the non-relativistic value: 5368.7 cm^{-1} [22]. Therefore, we have adopted the expressions (15) also for $Z > 50$. This type of fits was widely used by Edlén [19], as well as Curtis [20] in the analysis of isoelectronic sequences.

3.2 Range Z = 51–70

In this range, they are reported only the two levels with $J = 1$: ^{1}P$_1$ and ^{3}P$_1$, that decay to the fundamental ^{1}S$_0$. Missing values for ^{1}P$_1$ occur for $Z = 61, 65$ and 69, whereas missing values for ^{3}P$_1$ occur for $Z = 56$, 58, 59, 61, 62, 65, 67 and 69. Then, we follow these approaches:

1) For those values of Z when there are experimental values for both $J = 1$ levels, we constructed the matrix with $J = 1$ (Eq. (9)) with the values for $G^1_H(sp_-)$, $G^1_H(sp_+)$ and $R^1_H(sp_-, sp_+)$ given by equation (15). The values for $E_0(sp_-)$ and $E_0(sp_+)$ are found by diagonalizing that matrix.
   As an example, for $Z = 60$, where

$$E(^3\mathrm{P}_1) = 496\,857\ \mathrm{cm}^{-1}, \quad E(^1\mathrm{P}_1) = 829\,208\ \mathrm{cm}^{-1},$$

   and equations (15) gives

$$G^1(sp_-) = 208\,004\ \mathrm{cm}^{-1}, \quad G^1(sp_+) = 205\,548\ \mathrm{cm}^{-1}$$

   and

$$R^1(sp_-, sp_+) = 205\,884\ \mathrm{cm}^{-1},$$

   the solution of the system constituted by equations (11) and (10) gives us the values

$$E_0(sp_-) = 533\,082\,\mathrm{cm}^{-1} \text{ and } E_0(sp_+) = 793\,255\,\mathrm{cm}^{-1}.$$

Table 1. Compilation of the four levels of the $4s4p$ configuration of the Zn sequence, $Z = 30$–50, in cm^{-1}. Because all parameters $G^1(sp_-)$, $G^1(sp_+)$, $E_0(sp_-)$, $E_0(sp_+)$ and $R^1(sp_-, sp_+)$ can be recovered anallytically from the known experimental levels, it is not necessary to present them. The $J = 1$ levels were re-calculated with the use of the fitted $G^1(sp_-)$ and $G^1(sp_+)$ integrals, in order to show the goodness of that adjustments. The standard deviation is of the order of ± 28 cm^{-1}.

Z	^{1}P$_1$ (exp.)	^{1}P$_1$ (calc.)	^{3}P$_0$ (exp.)	^{3}P$_1$ (exp.)	^{3}P$_1$ (calc.)	^{3}P$_2$ (exp.)	References
30	46 745	46 761	32 311	32 501	32 497	32 890	[1]
31	70 700	70 651	47 370	47 816	47 872	48 750	[1]
32	91 873	91 817	61 733	62 496	62 513	64 138	[1]
33	112 022	111 994	75 812	76 962	76 987	79 492	[1]
34	131 733	131 736	89 749	91 350	91 392	94 960	[5]
35	151 289	151 293	103 593	105 712	105 750	110 624	[5]
36	170 835	170 843	117 389	120 094	120 123	126 553	[6]
37	190 502	190 500	131 157	134 523	134 533	142 802	[8]
38	210 378	210 365	144 933	149 029	149 014	159 433	[8]
39	230 529	230 502	158 709	163 607	163 584	176 474	[8]
40	251 031	251 009	172 535	178 305	178 271	194 009	[8]
41	271 939	271 898	186 363	193 077	193 034	212 033	[8]
42	293 333	293 281	200 311	207 982	207 935	230 642	[8]
44	337 727	337 688	228 244	238 118	238 124	269 736	[9]
45	360 810	360 778	242 262	253 346	253 390	290 277	[9]
46	384 718	384 649	256 490	268 745	268 809	311 648	[9]
47	409 312	409 274	270 621	284 251	284 258	333 853	[9]
48	434 699	434 660	284 831	299 825	299 819	356 855	[9]
49	460 878	460 896	299 171	315 530	315 539	380 737	[9]
50	488 338	488 288	313 704	331 470	331 500	405 823	[9]

2) For $Z = 56, 58, 59, 61, 62, 65, 67$ and 69, we use the values of equation (15) and the $E_0(sp_-)$ and $E_0(sp_+)$ values of the neighboring $Z's$ in order to find the missing parameters by interpolation.

Therefore, with the calculated values of $G^1_H(sp_-)$, $G^1_H(sp_+)$, $R^1_H(sp_-, sp_+)$, $E_0(sp_-)$ and $E_0(sp_+)$, the energies for the missing $J = 1$ levels, as well as the levels ^{3}P$_0$ and ^{3}P$_2$ follow from previous equations, and can be compared with theoretical estimations of references [29,30].

In order to compare our results (experimental and/or interpolated) with theoretical calculations of references [29,30], the summary is:

a) ^{1}P$_1$ levels: 17 values are experimental and 3 values were interpolated. The mean and standard deviation are

$$\Delta[(^1\mathrm{P}_{1,\mathrm{exp}}) - (^1\mathrm{P}_{1,Chen})] = (34 \pm 115)\ \mathrm{cm}^{-1};$$
$$\Delta[(^1\mathrm{P}_{1,\mathrm{exp}}) - (^1\mathrm{P}_{1,Hu})] = (-675 \pm 161)\ \mathrm{cm}^{-1}.$$

b) ^{3}P$_1$ levels: 12 values are experimental and 8 values were interpolated. The numbers are

$$\Delta[(^3\mathrm{P}_{1,\mathrm{exp}}) - (^3\mathrm{P}_{1,Chen})] = (-281 \pm 169)\ \mathrm{cm}^{-1};$$
$$\Delta[(^3\mathrm{P}_{1,\mathrm{exp}}) - (^3\mathrm{P}_{1,Hu})] = (113 \pm 195)\ \mathrm{cm}^{-1}.$$

c) ^{3}P$_0$ levels: all of them were calculated after the estimation of $G^1(sp_-)$, $G^1(sp_+)$, $R^1(sp_-, sp_+)$, $E_0(sp_-)$ and $E_0(sp_+)$ as explained above. Now,

$$\Delta[(^3\mathrm{P}_{0,\mathrm{exp}}) - (^3\mathrm{P}_{0,Chen})] = (-311 \pm 198)\ \mathrm{cm}^{-1};$$
$$\Delta[(^3\mathrm{P}_{1,\mathrm{exp}}) - (^3\mathrm{P}_{1,Hu})] = (372 \pm 242)\ \mathrm{cm}^{-1}.$$

d) ^{3}P$_2$ levels: the same situation as above. Now,

$$\Delta[(^3\mathrm{P}_{2,exp}) - (^3\mathrm{P}_{2,Chen})] = (373 \pm 459)\ \mathrm{cm}^{-1};$$
$$\Delta[(^3\mathrm{P}_{2,exp}) - (^3\mathrm{P}_{2,Hu})] = (986 \pm 300)\ \mathrm{cm}^{-1}.$$

Taking into account all levels,

$$\Delta[\mathrm{our} - -\mathrm{Ref.}\ [29]] = (-46 \pm 381)\ \mathrm{cm}^{-1}$$

and

$$\Delta[\mathrm{our} - -\mathrm{Ref.}\ [30]] = (210 \pm 662)\ \mathrm{cm}^{-1}.$$

This indicates that our values (experimental, interpolated and calculated) are in better agreement with reference [29] than with reference [30]. On the other hand, the comparison between the theoretical calculations indicates that Δ [Ref. [29]–Ref. [30]] $= (228 \pm 558)$ cm^{-1}.

3.3 Range Z = 70–92

In this range only the ^{1}P$_1$ level for some elements is reported, with several measurements due to different authors and different spectroscopic sources; in some cases, the values are discordating. As it was said above, we take the high-precision results from references [14,15] and not the laser-plasma measurements. In this range, it is not possible to derive values for $E_0\,(sp_-)$ and $E_0\,(sp_+)$ as in the previous subsection, due to the lack of the experimental ^{3}P$_1$ levels. We take, as the experimental data base, the latest works of Träbert et al. for $Z = 70, 74, 76, 78, 79, 82, 83, 90$ and 92 using the EBIT

source. We take into account that, in equation (12) the denominator

$$[E_0\,(sp_+) - E_0\,(sp_-)] + \left[G^1\,(sp_+) + G^1\,(sp_-)\right]/9$$

can be fitted in the range $Z = 30$–70 by the polynomial

$$\text{Denominator}\,(Z_c) = -96.8844 + 449.7958Zc + 104.0723Zc^2 + 1.5816Zc^3 + 0.1048Zc^4$$

with a correlation coefficient $R^2 = 1$. Then, for $Z = 70$, 74, 76, 78, 79, 82, 83, 90 and 92, we calculate $E_0(sp_+)$ from

$$E_0\,(sp_+) = E\left({}^1\mathrm{P}_1\right) - \frac{G^1\,(sp_+)}{9} - \frac{8\left[R^1\,(sp_-, sp_+)\right]^2/81}{\text{Denominator}\,(Z_c)} \quad (16)$$

with $G^1\,(sp_+)$ and $R^1\,(sp_-, sp_+)$ calculated from equation (15). After this, we interpolate for the other Zs in the range $Z = 70$–92. The results are shown in Table 3.

4 Comparison with theoretical values

Whereas the authors working with the non-relativistic codes, as the ones by Cowan [16] or Frose-Fischer [17] compare the theoretical Slater and spin-orbit integrals with the values deduced from the experiments, this is not so when using the fully-relativistic codes as the GRASP and HULLAC ones. We intend to make that comparison, using values of the GRASP code generated by ourselves.

Before commenting about the comparison between the theoretical and experimental values, we have noted the following interesting correlation between the theoretical values obtained by two independent codes: the one by Cowan [16] and the other one by Grant [18]: with high accuracy the relation

$$G^1\,(sp)\big|_{COWAN} \approx \frac{1}{3}\,G^1\,(sp_-)\big|_{GRASP} + \frac{2}{3}\,G^1\,(sp_+)\big|_{GRASP}\,;$$

is satisfied, practically the same theoretical relation given by equation (13).

Because it is known that, when using the Cowan codes, the relation between experimental and theoretical values for the Slater parameters is about 0.8–0.85 for high Z values [16], it is deduced that

$$G^1\,(sp_\pm)\big|_{exp} / \,G^1\,(sp_\pm)\big|_{GRASP} \approx 0.8{-}0.85$$

(or worse for lower Z values). Something similar occurs for the relation $R^1\,(sp_-, sp_+)\,|_{exp}/R^1\,(sp_-, sp_+)\,|_{GRASP}$.

5 Results and discussion

Summarizing, up to $Z = 50\,(Z_c = 21)$, where the four experimental level values are known, we calculate the five parameters: $E_0(sp_-)$, $E_0(sp_+)$, $G^1(sp_-)$, $G^1(sp_+)$ and $R^1(sp_-, sp_+)$ by fixing the relation

$$G^1(sp_-)/G^1(sp_+) = 1.012.$$

These values can be compared with theoretical ones, tending to approximately 0.80–0.85, as was said above. This range of Z is of great importance because the behavior of $G^1(sp_-)$, $G^1\,(sp_+)$ and $R^1(sp_-, sp_+)$ for all Z can be inferred, given by equations (15) (tending to be linear for high Z_c). In Table 1, we compile the four levels updating the Table 1 from reference [20]. Because all parameters $G^1(sp_-)$, $G^1(sp_+)$, $E_0(sp_-)$, $E_0(sp_+)$ and $R^1(sp_-, sp_+)$ can be recovered anallytically from the known experimental levels, it is not necessary to present them explicitly (see Sect. 3.1).

In the range $Z = 51$–70, missing ${}^1\mathrm{P}_1$ level occurs for $Z = 61$, 65 and 69 whereas missing ${}^3\mathrm{P}_1$ level occurs for $Z = 56$, 58, 59, 61, 62, 65, 67 and 69. For $Z = 51$–55, 57, 60, 63, 64, 66 and 68, where the two $J = 1$ levels are known, we calculated $E_0(sp_-)$ and $E_0(sp_+)$ by diagonalizing the matrix 9, with $G^1(sp_-)$, $G^1(sp_+)$ and $R^1(sp_-, sp_+)$ given by equations (15). Therefore, using judicious interpolation, we estimated $E_0(sp_-)$ and $E_0(sp_+)$ for all range of Z. Then, we proposed also the approximate values for $J = 0, 2$; all levels are presented in Table 2a. The four levels, for $Z = 30 - 70$, are shown in Figure 1. For $Z = 51 - 69$, the comparison with the large scale calculations from Chen and Cheng [29] and Hu et al. [30] are shown in Figures 2a and 2b. Our interpolated values are close, in general, to the calculated values from Chen and Cheng rather than the results from Hu et al. [30] In general, the greater discrepance is for the ${}^3\mathrm{P}_2$ levels. On the other hand, it is interesting to note the bad calculation of these authors for ${}^3\mathrm{P}_1(Z = 70)$: whereas the measurement of Hinnov et al gives 674 832 cm^{-1}, Chen and Cheng gives 676 338 cm^{-1}. In Table 2b, we present the interpolated $J = 1$ levels of Table 2a, compared with

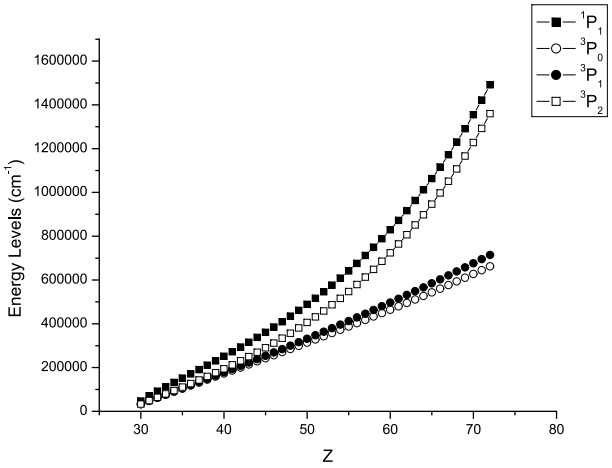

Fig. 1. The four levels of the $4s4p$ configuration of the Zn isoelectronic sequence for $Z = 30$–70 (see the text to distinguish between experimental from the interpolated values). Note the strong departure from the linearity of levels ${}^1\mathrm{P}_1$ and ${}^3\mathrm{P}_2$ for $Z \gtrsim 50$.

Table 2a. The four levels of the $4s4p$ configuration of the Zn sequence, $Z = 51$–72, in cm^{-1}. The $J = 1$ levels are in general experimental, although in several cases we interpolate, as it is explained in the text. The levels $^3P_0$ and $^3P_2$ are calculated as explained in the text. The uncertainties in the experimental levels correspond to uncertainties in the wavelength measurements of $\Delta\lambda \sim 0.01$ Å for the transitions to the ground level $4s^2\ ^1S_0$ (see, for example, Ref. [12] although lesser uncertainties are reported in Ref. [14]).

Z	$^1P_1$ (exp. or int.)	$^3P_0$ (calc.)	$^3P_1$ (exp. or int.)	$^3P_2$ (calc.)	References
51	516 569 ± 27	328 166	347 425 ± 12	431 833	[3]
52	545 962 ± 30	342 782	363 524 ± 13	458 978	[3]
53	576 442 ± 33	357 505	379 744 ± 14	487 223	[12]
54	608 228 ± 37	372 319	396 082 ± 16	516 802	[12]
55	641 276 ± 41	387 260	412 558 ± 17	547 652	[12]
56	675 804 ± 46	402 290	429 141	580 002	[12]; $^3P_1$ interpolated
57	711 814 ± 51	417 417	445 831 ± 20	613 845	[7]
58	749 333 ± 56	432 731	462 710	649 196	[12]; $^3P_1$ interpolated
59	788 389 ± 62	448 187	479 728	686 084	[3]; $^3P_1$ interpolated
60	829 208 ± 69	463 748	496 857 ± 25	724 739	[12]
61	871 896	479 565	514 242	765 264	$^1P_1$ and $^3P_1$ interpolated
62	916 506 ± 84	495 289	531 542	807 718	[12]; $^3P_1$ interpolated
63	963 094 ± 93	511 019	548 847 ± 30	852 150	[12]
64	1 011 828 ± 102	526 850	566 251 ± 32	898 727	[12]
65	1 062 720	543 122	584 415	947 447	$^1P_1$ and $^3P_1$ interpolated
66	1 116 071 ± 125	560 072	602 580 ± 36	998 615	[10]
67	1 172 182 ± 137	576 817	620 883	1 052 550	[12]; $^3P_1$ interpolated
68	1 229 967 ± 151	593 425	639 031 ± 41	1 108 145	[12]
69	1 290 868	609 850	657 004	1 166 864	$^1P_1$ and $^3P_1$ interpolated
70	1 354 885 ± 184	626 126	674 832 ± 68	1 228 701	[14],[7]

Table 2b. The interpolated $J = 1$ levels of the previous table, compared with the theoretical calculations of reference [29]. Note that there is a noticeable discrepance only for the $^3P_1$ case for $Z = 69$ (see the Text).

Z	$^1P_1$	$^1P_1$ (Ref. [29])	$\Delta\sigma$ (int. – Ref. [29])	$^3P_1$	$^3P_1$ (Ref. [29])	$\Delta\sigma$ (int. – Ref. [29])
56				429 141	429 406	−249
58				462 710	462 990	74
59				479 728	479 976	104
61	871 896	871 877	11	514 242	514 343	−197
62				531 542	531 732	−252
65	1 062 720	1 062 706	14	584 415	584 771	−356
67				620 883	620 880	3
69	1 290 868	1 291 039	−171	657 004	657 691	−687

the theoretical calculations of reference [29]. Note that there is a noticeable discrepance for the $^3P_1$ case only for $Z = 64$ and 69 (but, see the previous sentence about the calculations for $Z = 70$). With respect to the $^1P_1$ levels, the comparison between the theoretical calculations [29,30] and the predicted measurements [12], would indicate that for $Z = 67$ that measurement is possibly wrong.

In the range $Z = 70$–92, where only the $^1P_1$ levels for $Z = 70$, 74, 76, 78, 79, 82, 83, 90 and 92 were measured, we calculated $E_0(sp_+)$ from equation (16) and interpolated for the other values of Z. Missing $^1P_1$ values were calculated using equation (12). The values for $E_0(sp_+)$ and $E(^1P_1)$ are shown in Table 3, where they are compared with the calculation by Chen and Cheng [29]. Note that the greater discrepance, $\Delta\sigma = 859$ cm^{-1} for $Z = 87$, is equivalent to $\Delta\lambda \simeq 0.009$ Å (the order of the measurement accuracy). The analysis of the experimental, as well as our interpolations and Chen and Cheng calculations indicates that

$$\Delta\left[\left(^3P_{2,exp}\right) - \left(^3P_{2,ours}\right)\right] = (57 \pm 238)\ \text{cm}^{-1}$$

whereas

$$\Delta\left[\left(^3P_{2,exp}\right) - \left(^3P_{2,Chen}\right)\right] = (99 \pm 254)\ \text{cm}^{-1}.$$

These results indicate that the interpolation procedure give values of comparable accuracy as the large-scale calculations.

Concerning to the self-energy approximate estimates, the equation (14) is, explicitly

$$\begin{aligned}\left[E\left(4p_{1/2}\right) - E\left(4p_{3/2}\right)\right]_{SE} &= 10.884 \times 10^{-3} Z_{\text{eff}}^4 \\ &+ 2.88 \times 10^{-10} Z_{\text{eff}}^7 \\ &- 3.124 \times 10^{-12} Z_{\text{eff}}^8; \quad (17)\end{aligned}$$

with Z_{eff} values inferred from the expectation values for $\langle r\rangle$, $\langle r^2\rangle$ and $\langle 1/r\rangle$ given by the GRASP code. The values given by equation (17) are shown, jointly with the Chen and Cheng calculations in Figure 3.

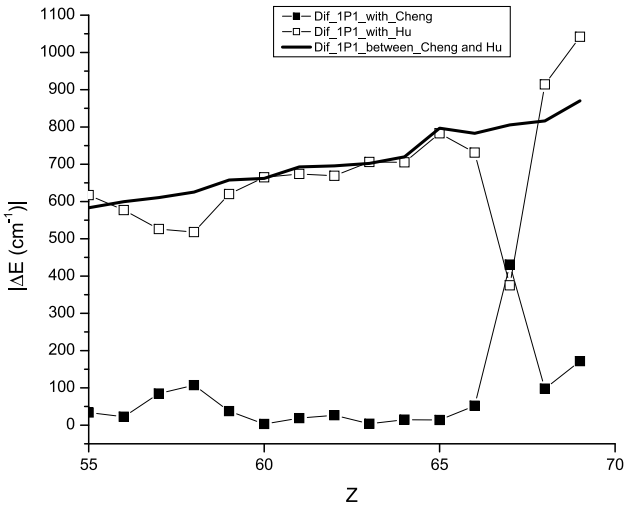

(a)

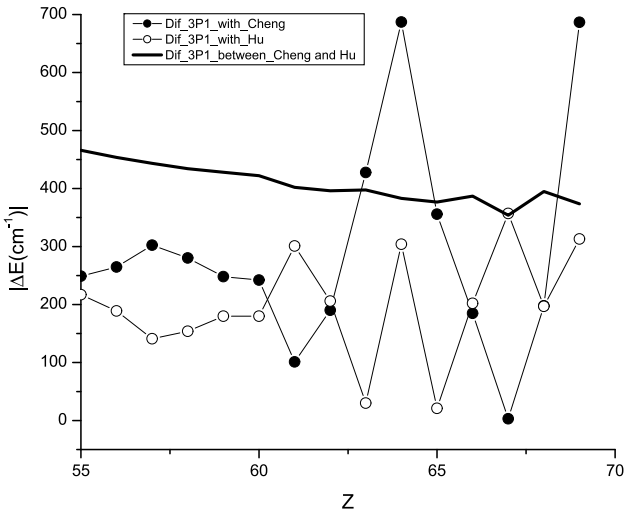

(b)

Fig. 2. (a) Difference between our established levels ^{1}P$_1$ and the values of the large-scale relativistic calculations from Chen and Cheng [29] and Hu et al. [30] for $Z = 51$–69 ($Z_c = 22$–40). (b) Difference between our established levels ^{3}P$_1$ and the values of the large-scale relativistic calculations from Chen and Cheng [29] and Hu et al. [30] for $Z = 51$–69 ($Z_c = 22$–40).

6 Conclusions

The specific purposes of this work were: 1) to compare the experimentally deduced Slater parameters and those provided by the GRASP code, 2) to use the capability of the semi-empirical method for interpolation, extrapolation and consistency checking.

Concerning item 1, we parametrized completely the $4s4p$ levels belonging to the Zn isoelectronic sequence up to $Z = 50$, by using the *Relativistic jj-coupling approach*, and the experimentally derived parameters were compared with those obtained with the GRASP code. In this range, it was verified that the relation between the experimental values of $G^1(sp_-)$, $G^1(sp_+)$ and $R^1(sp_-, sp_+)$

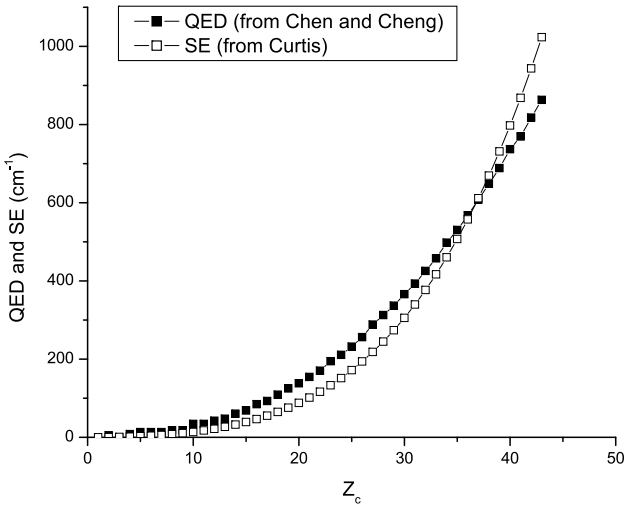

Fig. 3. Self-energy estimations from the Curtis expression (*only SE*) as compared with *all* QED calculations from reference [29].

and their theoretical counterparts followed the empirical laws given by:

$$G^1\,(sp_\pm)\big|_{exp} \,/\, G^1\,(sp_\pm)\big|_{GRASP}$$
$$\approx R^1\,(sp_-, sp_+)\big|_{exp} \,/\, R^1\,(sp_-, sp_+)\big|_{GRASP} \approx 0.8 - 0.85.$$

For the item 2, we estimated by interpolation, in the range $Z = 51$–70, the ^{1}P$_1$ level for $Z = 61, 65$ and 69 and the ^{3}P$_1$ level for $Z = 56$, 58, 59, 61, 62, 65, 67, 69 and 71 establishing, therefore, the $J = 1$ level values for this interval of Z. Also, approximate values for levels with $J = 0$, 2, where experimental values were not available, were presented.

The entire range $Z = 30$–70 allowed to fit the values of $[E_0\,(sp_+) - E_0\,(sp_-)] + \left[G^1\,(sp_+) + G^1\,(sp_-)\right]/9$ with a very high correlation coefficient. This fact was essential to find very approximate values of $E_0\,(sp_+)$ for $Z = 72$–92 implying that ^{1}P$_1$ could be estimated in definitive, for $Z = 30$–92.

From the comparison between experimental and theoretical values it results that both codes, the one by Cowan, using the quasi-relativistic approach and the other one by Grant, using the fully-relativistic point of view, are of similar quality for interpretating this isoelectronic sequence. The comparison between our experimentally derived (or interpolated) values and the large-scale relativistic calculations by Chen and Cheng [29] and Hu et al. [30] indicates that the comparison is good, in general, for the levels with $J = 1$, except for $Z = 69$. In short, our work indicates that the semi-empirical treatment of the Zn isoelectronic sequence using the *jj-relativistic approach* gives values for the missing levels of equivalent quality as the large-scale relativistic configuration-interaction approach of Chen and Cheng [29] and Hu et al. [30].

It is important to remark that for the range $Z = 51$–70, and for 80 values (4 levels times 20 ions),

$$\Delta\,[\text{our–Ref. [29]}] = (-46 \pm 381)\ \text{cm}^{-1}$$

Table 3. The $^1P_1$ levels in the range $Z = 70$–92: they are (i) the experimental, (ii) the calculated as explained in the text and (iii) the theoretical from reference [29]. Also, the $E_0\,(sp_+)$ values are shown. Note that the greatest discrepance, $\Delta\sigma = 859$ cm^{-1} for $Z = 87$ is equivalent to $\Delta\lambda \simeq 0.009$ Å (the order of the measurement accuracy).

Z	$^1P_1$ (exp)	$E_0\,(sp_+)$	$^1P_1$ (calc)	$^1P_1$ (Ref. [29])	$\Delta\sigma$ (calc – Ref. [29])
70	1 354 885	1 314 596	1 354 885	1 354 923	–23
73		1 523 824	1 564 695	1 564 716	–21
74	1 641 228	1 600 029	1 641 159	1 641 258	–99
75		1 679 990	1 721 518	1 721 349	169
76	1 805 576	1 763 637	1 805 264	1 805 150	114
77		1 850 840	1 892 956	1 892 903	53
78	1 984 521	1 941 807	1 984 789	1 984 689	100
79	2 080 806	2 037 693	2 080 952	2 080 749	203
80		2 138 117	2 181 637	2 181 165	472
81		2 243 099	2 287 035	2 286 421	614
82	2 397 018	2 352 661	2 396 890	2 396 435	455
83	2 511 610	2 466 824	2 511 621	2 511 611	10
84		2 586 430	2 631 650	2 632 110	–460
85		2 711 734	2 757 397	2 758 094	–697
86		2 842 993	2 889 104	2 889 885	–781
87		2 980 461	3 027 027	3 027 886	–859
88		3 124 395	3 171 421	3 172 259	–838
89		3 275 050	3 322 543	3 323 327	–784
90	3 480 646	3 432 682	3 480 732	3 480 766	–34
91		3 597 546	3 645 987	3 646 594	–607
92	3 818 820	3 769 898	3 818 309	3 818 632	–323

and

$$\Delta\,[\text{our–Ref. [30]}] = (210 \pm 662)\ \text{cm}^{-1}.$$

On the other hand, the comparison between the theoretical calculations indicates that

$$\Delta\,[\text{Ref. [29]–Ref. [30]}] = (228 \pm 558)\ \text{cm}^{-1}.$$

These values indicate that our approach produced values of comparable quality as the theoretical ones.

With respect to the non-relativistic treatment given by reference [20], it is important to note: (i) the use of the spin-orbit integral ζ_{np} in that formulation and (ii) the empirical linearity of the screening parameters S_i (S_G and S_ζ) in terms of $1/(Z - S_i)$ in the range $Z = 30$–50. As we can see in equation (3), the calculation of ζ_{np} needs the energies of the $^3P_2$ and $^3P_0$ levels, but these levels are unknown for $Z > 50$. Therefore, the method of reference [20] is not possible for $Z > 50$. Moreover, as can be inferred from our Table 2a, the behavior of the screening parameters S_i in terms of $1/(Z - S_i)$ are strongly non-linear in the range $Z = 51$–70. Therefore, summing all, the extrapolations from the range $Z = 30$–50 to $Z > 50$ are, in our opinion, not possible using the non-relativistic approach. These facts were the trigger for our present work.

The comments about the manuscript by Dr. Darío Mitnik (Instituto de Astronomía y Física del Espacio, Buenos Aires) as well as the comments and articles sent to us by Dr. E. Träbert (Astronomisches Institut, Ruhr-Universität Bochum, Bochum, Germany) are gratefully acknowledged. The interest and correspondence with Prof. L.J. Curtis, from University of Toledo are, also, gratefully acknowledged. The support from the CONICET, Universidad Nacional del Centro, Autoridad Regulatoria Nuclear and Comisión de Investigaciones Científicas de la Provincia de Buenos Aires (all of them from Argentina) are strongly acknowledged. The comments and suggestions of the two referees of this work are gratefully acknowledged.

References

1. http://www.nist.gov/PhysRevData/ASD/levels
2. J. Reader, G. Luther, Phys. Rev. Lett. **45**, 609 (1980)
3. N. Acquista, J. Reader, J. Opt. Soc. Am. B **1**, 649 (1984)
4. B. Isberg, U. Litzén, Phys. Scripta **31**, 533 (1985)
5. Y.N. Joshi, Th.A.M. van Kleef, Phys. Scripta **34**, 135 (1986)
6. A. Trigueiros, S.-G. Petterson, J.G. Reyna Almandos, Phys. Scripta **34**, 164 (1986)
7. E. Hinnov et al., Phys. Rev. A **35**, 4876 (1987)
8. U. Litzén, J. Reader, Phys. Rev. A **36**, 5159 (1987)
9. S.S. Churilov, A.N. Ryabtsev, Phys. Scripta **38**, 326 (1988)
10. J. Sugar, V. Kaufman, D.H. Baik, Y.-K. Kim, J. Opt. Soc. Am. B **8**, 1795 (1991)
11. A.N. Ryabtsev et al., Phys. Scripta **48**, 326 (1993)
12. C.M. Brown et al., At. Data Nucl. Data Tables **58**, 203 (1994)
13. S.S. Churilov, Y.N. Joshi, J. Opt. Soc. Am. B **13**, 11 (1996)
14. E. Träbert, P. Beiersdorfer, H. Chen, Phys. Rev. A **70**, 032506 (2004)
15. E. Träbert, J. Clementson, P. Beiersdorfer, J.A. Santana, Y. Ishikawa, Phys. Rev. A **82** , 062519 (2010)

16. R.D. Cowan, *The Theory of Atomic Structure and Spectra* (University of California Press, Berkeley, 1981)
17. C. Froese Fischer, T. Brage, P. Jönsson, *Computational Atomic Structure, an MCHF Approach* (Institute of Physics Publishing, Bristol, 1997)
18. I.P. Grant, *Relativistic Quantum Theory of Atoms and Molecules* (Springer Science, New York, 2007)
19. B. Edlen, "Atomic Spectra" in *Handbuch der Physik* (Springer, Berlin, 1964), Vol. 27, p .80
20. L.J. Curtis, *Atomic Structure and Lifetimes* (Cambridge University Press, Cambridge, 2003)
21. L.J. Curtis, J. Opt. Soc. Am. B **2**, 407 (1985)
22. E.U. Condon, H. Odabasi, *Atomic Structure* (Cambridge University Press, Cambridge, 1980)
23. L.J. Curtis, J. Opt. Soc. Am. B **3**, 1102 (1986)
24. H.O. Di Rocco, Rev. Mex. Física **48**, 76 (2002)
25. B.W. Shore, D.H. Menzel, *Principles of Atomic Spectra* (John Wiley, New York, 1968)
26. A. de-Shalit, I. Talmi, *Nuclear Shell Theory* (Academic Press, New York, 1963)
27. F.P. Larkins, J. Phys. B **9**, 37 (1976)
28. W.R. Johnson, *Atomic Structure Theory* (Springer Verlag, Berlin, 2007)
29. M.H. Chen, K.T. Cheng, J. Phys. B **43**, 074019 (2010)
30. F. Hu, J. Yang, C. Wang, X. Zhao, H. Zang, G. Jiang, At. Data Nucl. Data Tables **98**, 301 (2012)
31. L.J. Curtis, J. Phys. B **18**, L651 (1985)